1
2 Carbon consequences of forest disturbance and recovery across the conterminous
3 United States
4

5 **Authors:** Christopher A. Williams[1,*], G. James Collatz[2], Jeffrey Masek[2], Samuel N. Goward[3]
6 [1]Graduate School of Geography, Clark University, Worcester, MA, USA
7 [2]NASA Goddard Space Flight Center - Code 618, Biospheric Sciences Laboratory, Greenbelt,
8 MD, USA
9 [3]Department of Geography, University of Maryland, College Park, MD, USA
10 *Corresponding Author: cwilliams@clarku.edu, P: 508-793-7323; F: 508-793-8881

11

18
19
20

21 **Abstract:**

22 Forests of North America are thought to constitute a significant long term sink for atmospheric

23 carbon. The United States Forest Service Forest Inventory and Analysis (FIA) program has

24 developed a large data base of stock changes derived from consecutive estimates of growing stock

25 volume in the US. These data reveal a large and relatively stable increase in forest carbon stocks

26 over the last two decades or more. The mechanisms underlying this national increase in forest

27 stocks may include recovery of forests from past disturbances, net increases in forest area, and

28 growth enhancement driven by climate or fertilization by CO_2 and Nitrogen. Here we estimate

29 the forest recovery component of the observed stock changes using FIA data on the age structure

30 of US forests and carbon stocks as a function of age. The latter are used to parameterize forest

31 disturbance and recovery processes in a carbon cycle model. We then apply resulting

32 disturbance/recovery dynamics to landscapes and regions based on the forest age distributions.

33 The analysis centers on 28 representative climate settings spread about forested regions of the

34 conterminous US. We estimate carbon fluxes for each region and propagate uncertainties in

35 calibration data through to the predicted fluxes. The largest recovery-driven carbon sinks are

36 found in the Southcentral, Pacific Northwest, and Pacific Southwest regions, with spatially

37 averaged net ecosystem productivity (*NEP*) of about 100 g C m^{-2} a^{-1} driven by forest age

38 structure. Carbon sinks from recovery in the Northeast and Northern Lake States remain

39 moderate to large owing to the legacy of historical clearing and relatively low modern disturbance

40 rates from harvest and fire. At the continental scale, we find a conterminous U.S. forest *NEP* of

41 only 0.16 Pg C a^{-1} from age structure in 2005, or only 0.047 Pg C a^{-1} of forest stock change after

42 accounting for fire emissions and harvest transfers. Recent estimates of *NEP* derived from

43 inventory stock change, harvest, and fire data show twice the *NEP* sink we derive from forest age

44   distributions. We discuss possible reasons for the discrepancies including modeling errors and

45   the possibility of climate and/or fertilization (CO_2 or N) growth enhancements.

46

1. Introduction

The global imbalance among ocean, industrial, and land use sources/sinks of CO_2 and the amount accumulating in the atmosphere implies significant net CO_2 uptake by the terrestrial biosphere [e.g. *Schimel et al.*, 2001; *Tans et al.*, 1990]. Despite large uncertainty about magnitude and process, analyses tend to point to northern temperate and boreal lands as dominant terrestrial sinks of CO_2 but with considerable controversy regarding attribution to specific regions or continents [e.g. *Bousquet et al.*, 2000; *Fan et al.*, 1998; *Gurney et al.*, 2002; *Kaminski et al.*, 2001; *Myneni et al.*, 2001; *Tans et al.*, 1990]. However, some recent work suggests far smaller sinks in northern temperate and boreal lands [*Ito et al.*, 2008; *Stephens et al.*, 2007; *Yang et al.*, 2007].

Estimates of the conterminous U. S. forest net carbon uptake from the atmosphere range from only 10 to over 200 Tg C a^{-1} [*EPA*, 2010; *Houghton et al.*, 1999; *King et al.*, 2007; *Pacala et al.*, 2001; *Turner et al.*, 1995] in the last 2 decades. Note that here we consider the forest stock change alone rather than the forest sector stock change, where the latter also includes carbon accumulated in wood products (see State of the Carbon Cycle Report [*King et al.*, 2007]).

Techniques for estimating forest carbon fluxes at regional to national scales include three approaches. The stock change method is exemplified in the US report to the United Nations Framework Convention for Climate Change [e.g. *EPA*, 2008] which uses US Forest Service Forest Inventory and Analysis (FIA) data on sequential measurement of tree diameters and/or wood volumes for about 100,000 forest plots at 5-20 year intervals. Allometric and biomass expansion factors are used to convert volume into forest carbon stocks. The rate of carbon uptake

68   is then estimated as the difference between sequential measurements divided by the number of

69   years in the interval.

70   Another technique for estimating forest carbon sinks combines estimates of the stand age

71   structure of forests with age-specific carbon accumulation rates, termed the "age-accumulation"

72   approach in this work. These carbon accumulation rates are inferred from carbon stocks as a

73   function of age [e.g. *Houghton*, 1999], known as yield tables in forestry literature, and may be

74   derived empirically from inventory estimates of stand volume and age or from a process oriented

75   dynamic growth model. Finally, forest carbon sinks have been estimated from process models

76   that account for the effects of climate variability and CO_2 and nitrogen fertilization but not

77   necessarily for land use and disturbance processes [e.g. *Schimel et al.*, 2000]. These effects are

78   fully contained in the stock change method because it relies on contemporary changes in stocks,

79   but the age-accumulation approach relies on a historical characterization of carbon stock

80   accumulation and thus misses some of the contemporary influences (see Auxiliary 4).

81   Forest stock changes result from the sum of net ecosystem productivity (*NEP*), fire losses, and

82   harvest (see Figure 1). Significant decreases in harvest and fire have not been observed over the

83   past few decades so speculation as to the mechanisms underlying the stock increases have focused

84   more on growth enhancement from either climate change or fertilization with elevated carbon

85   dioxide or nitrogen [*Houghton*, 1999; *McGuire et al.*, 2001; *Nemani et al.*, 2002; *Pan et al.*, 2009;

86   *Schimel et al.*, 2000; *Zhou et al.*, 2003] and on forest growth from post-disturbance recovery or

87   fire suppression [*Caspersen et al.*, 2000; *Hurtt et al.*, 2002; *Pacala et al.*, 2001]. Though the

88   growth enhancement hypothesis has been challenged by *Casperson et al.* [2000] using forest

89   inventory data, others have argued that plausible rates of growth enhancement cannot be detected

90   using existing inventories [*Joos et al.*, 2002] and recent work presents observational evidence

91 supporting a large climate change or fertilization induced sink [*Cole et al.*, 2010; *McMahon et al.*,

92 2010; *Thomas et al.*, 2009].

93   Disturbed forests, if not converted to another land cover type, have the potential to regrow,

94 recover, or even surpass pre-disturbance carbon stocks over decades to several hundred years.

95 The long-standing dogma of the carbon source/sink dynamics for stand-replacing disturbance

96 involves a rapid pulse emission followed by sizeable net uptake that gradually declines [*Koerner*,

97 2003; *Odum*, 1969]. This pattern is broadly supported by chronosequence observations of carbon

98 stocks [*Bond-Lamberty et al.*, 2004; *Gough et al.*, 2007; *Pregitzer and Euskirchen*, 2004; *Richter*

99 *et al.*, 1999; *Thornton et al.*, 2002] and forest-atmosphere net CO_2 exchange [*Amiro et al.*, 2011;

100 *Barford et al.*, 2001; *Goulden et al.*, 2011; *Law et al.*, 2003; *Schwalm et al.*, 2007], but the precise

101 post-disturbance carbon dynamics vary by forest type and climate and this detail remains poorly

102 characterized.

103   The analysis reported here attempts comprehensive assessment of the carbon consequences of

104 past and present forest disturbance and recovery across the conterminous United States. We ask

105 if the forest age structure of the conterminous US forests accounts for the stock changes reported

106 by the FIA. Our approach utilizes the national forest inventory data (and uncertainties) to

107 constrain the forest disturbance and recovery processes represented in an ecosystem carbon cycle

108 model to obtain regional and national estimates of carbon consequences. The basic method can

109 be described as having two main steps. First, we derive forest type and climate specific post-

110 disturbance *NEP* trajectories by fitting a first-order terrestrial carbon cycle model (CASA, [*Potter*

111 *et al.*, 1993; *Randerson et al.*, 1996]) to grow wood stocks consistent with FIA data. Second,

112 these characteristic trajectories are applied to landscapes with forest age maps obtained from FIA

113 age distributions to derive maps of *NEP* and biomass. As such, our approach corresponds to the

114   age-accumulation method for estimating forest carbon sinks as described above. Results

115   represent carbon dynamics of forested ecoregions across the conterminous US to provide a

116   continental-scale view of forest recovery from past disturbances. In addition, we formally

117   propagate the uncertainty in FIA age-biomass trends using a Monte Carlo approach, as well as

118   examine to what degree results are sensitive to uncertainty in the model's parameterization of

119   carbon turnover time, and dependence on light, moisture, and temperature. Discrepancies

120   between FIA estimates of stock changes and those from our age-accumulation modeling are

121   assessed in terms of modeling errors and potential growth enhancements above and beyond

122   recovery, similar to *Houghton* [2003].

123

2. Methods

125   **2.1 Overview**

126   The core of our approach is to estimate the frequency (F) of land area in a region (A_{reg}), as

127   well as the flux or stock of carbon (Q) each within strata of stand age, forest type (e.g. Aspen-

128   Birch), and site productivity (high or low) (denoted with a, f, p subscripts). Regions are defined

129   according to the Resource Planning Act Assessment by the US Forest Service. From this we

130   calculate the regional mass flux or stock ($Q_{reg,s}$) for a particular climate setting (subscript s) within

131   each region, as well as its uncertainty (δ, described further below), according to

132

$$Q_{reg,s} = \sum_a \sum_f \sum_p Q_{afp} F_{afp} A_{reg}$$

134   (1),

135

136   where F is the frequency of forest area adjusted to sum to unity over the three strata and obtained

137   from the regional FIA samples of the area of forest land as described in Section 2.2, A_{reg} is the

138   total forested area in the region, and subscripts are: a for stand age, f for forest type group, and p

139   for productivity class. The work reported here is part of a larger project to incorporate stand age

140   derived from Landsat time series data. In this parallel effort, specific scenes for Landsat time

141   series were obtained from a statistically rigorous sampling procedure of forest type spatially

142   dispersed within Eastern and Western regions [*Goward et al.*, 2008]. Here we use the climate

143   (temperature, precipitation, incident solar radiation) and phenology for each scene (Figure 2) to

144   simulate fluxes and stocks for each forest type and productivity class within the scene. The scenes

145   within a region are generally good representations of the region except for the Pacific Southwest

146   where coastal forests are not well represented. The scene level fluxes are then aggregated to

147   regional forest fluxes and stocks by averaging across the number of climate settings (scenes, N_s)

148   in a region as

149

150
$$Q_{reg} = \frac{1}{N_s} \sum_s Q_{reg,s}$$
$$\delta Q_{reg} = \frac{1}{N_s} \sum_s \delta Q_{reg,s}$$
(2),

151

152   and conterminous US estimates (subscript *nat*) are obtained from the sum over regions

153

154
$$Q_{nat} = \sum_{reg} Q_{reg}$$
$$\delta Q_{nat} = \sum_{reg} \delta Q_{reg}$$
(3).

155

156   We note that our estimates do not account for possible changes in forest carbon due to changes in

157   forest area, though in the Discussion section we explain why this is unlikely to contribute a large

158   carbon source or sink given the rates of current-day net land conversion.

159   The relationship between fluxes and stocks can be diagramed as shown in Figure 1. The so-

160   called forest sector sources/sinks refer to the net flux between the atmosphere and forest stocks

161   plus wood products stocks. The inventory approach to calculating the net forest-atmosphere flux

162   involves a measured change in carbon stocks over a specified period. A change in forest carbon

163   stocks can occur because of changes in the physiological fluxes of photosynthesis and ecosystem

164   respiration (balanced as *NEP*), as well as changes in disturbance for example by fire or harvest.

165   *NEP* can then be inferred as the difference between ΔC_{stocks} and removals from fire and harvest.

166   The net forest sector flux to the atmosphere is the sum of ΔC_{stocks} and $\Delta C_{wood\ products}$. This

167   approach, used in national reports to United Nations Framework Convention on Climate Change,

168   derives $\Delta C_{wood\ products}$ from independent harvest records and empirical decay constants for wood

169   products and landfills.

170   Our approach is to calibrate our modeled biomass as a function of age using forest inventory

171   data. We then apply the biomass and associated *NEP* from forest disturbance and recovery to the

172   landscape based on the forest area reported by the FIA within strata of age, forest types and

173   productivity classes within each region. In our modeling framework an important driver of

174   ΔC_{stocks} is net primary production (*NPP*), and the turnover times of wood and detrital pools. *NPP*

175   allocated to leaves and fine roots is quickly decomposed and cannot represent a persistent (>

176   decadal) sink. The turnover rates of wood and its immediate detrital pool, coarse woody debris,

177   are much slower, on the order of decades, and thus able to account for long-term net carbon fluxes

178   (on the order of a century). Fluxes from large stocks of slowly overturning soil pools are also

179   slow to respond to disturbance. By the time these large soil pools are affected by disturbance,

180   recovery may have already occurred. This phenomenon is expressed as a low sensitivity of *NEP*

181   to the slow turnover pools in recovering forests (see Auxiliary Material, Auxiliary 1). Of course

182   the slow soil pools are a significant source or sink in conditions where changes in fluxes into the

183   slow pools are large and longer term such as in permanent conversion from or to forest. This

184   approach allows us to map *NEP* from recovery, one of the key atmospheric flux components

185   needed to understand source/sink processes. *NEP* is a purely biological flux dependent on

186   photosynthesis and respiration alone. Fluxes out of the forest arising from harvest or fire combine

187   with *NEP* to produce net biome productivity (*NBP*) which is equivalent to ΔC_{stocks}. Note that we

188   have neglected the generally smaller fluxes that contribute to *NBP* such as lateral fluxes of

189   carbonate and organic matter in liquid form as well as volatile organic carbon emissions (see

190   *Chapin III et al.* [2006]).

191

192   **2.2 Data Sources and Modeling**

193   Flux trajectories are derived by fitting forest growth, mortality and shedding, and allocation

194   parameters within the Carnegie-Ames-Stanford Approach (CASA) carbon-cycle process model

195   [*Potter et al.*, 1993; *Randerson et al.*, 1996] to accumulate carbon in aboveground wood biomass

196   consistent with forest inventory data. Productivity in CASA is represented with a light use

197   efficiency approach in which *NPP* is proportional to the fractional absorption of

198   photosynthetically active radiation (f_{PAR}) times an efficiency term modulated by environmental

199   conditions. *NPP* is allocated to leaves, roots, and wood which have specific turnover rates that

200   reflect the delivery of carbon to nine detrital pools on the surface and in the soil. These pools

201   decompose at specific turnover rates that are also modulated by environmental conditions.

202   Disturbance causes *NPP* to initially decrease, and removes or transfers carbon between live and

203   detrital pools, the atmosphere, and forest harvest. In this implementation, we adjust the default

204   rate of productivity to match carbon accumulation observed in age-accumulation trajectories from

205   forest inventory data.

206   Inventory data were obtained from the FIA field plots (FIA Database Version 4), providing

207   means and sampling errors for two attributes: 1) all live, oven-dry aboveground wood biomass,

208   and 2) area of forest land. The quotient of these attributes provides biomass per unit area. Each

209   attribute was sampled within strata of forest type group (28 classes), age (20 year age classes to

210   200+ years), and lumped into high and low productivity classes, defined as 120 to >225 cubic feet

211   acre^{-1} annum^{-1} and 20 to <120 cubic feet acre^{-1} annum^{-1} respectively. Inventory samples were

212   drawn for regions defined by the Resource Planning Act Assessment by the US Forest Service

213   that divides the conterminous U.S. into the Northeast (NE), Southeast (SE), Northern Lakes States

214   (NLS), South Central (SC), Northern Prairie States (NPS), Rocky Mountain North (RMN), Rocky

215   Mountain South (RMS), Pacific Southwest (PSW), and Pacific Northwest (PNW) region (Figure

216   2). FIA data on forest carbon and area that are available via World Wide Web download include

217   variances for each. However these variances cannot be exactly combined to estimate uncertainty

218   because of unknown covariance between carbon stock and area [*Bechtold and Patterson*, 2005].

219   Statisticians from the FIA (Charles Scott and colleagues, USFS National Inventory and

220   Monitoring Applications Center) processed the national plot data to provide our study with

221   custom products that we employed in this analysis, namely the aboveground live wood biomass

222   per unit area and its variance for each major forest type, age cohort, productivity class, for each

223   region shown in Figure 2. We confirmed that the data in this custom delivery were nearly

224   identical to those obtained from other web-based data servers maintained and made available by

225   the FIA.

226   For this implementation we drive the CASA model with the f_{PAR} from a smoothed version of

227   the MODIS MOD15A2 product [*Nightingale et al.*, 2009] for each forest type group as well as

228   climatological seasonality of monthly weather using NASA Goddard Institute of Space Sciences

229   (GISS) air temperature anomalies [*Hansen et al.*, 1999] added to a temperature climatology

230   [*Leemans and Cramer*, 1991], GISS solar radiation [*Zhang et al.*, 2004], and Global Precipitation

231   Climatology Project (GPCP) precipitation [*Adler et al.*, 2003]. These meteorological driver data

232   were sampled at the 1-degree scale while f_{PAR} was provided at 1 km resolution then averaged for

233   each forest type within each of the 28 simulation climate domains. As such, we obtain carbon

234   flux trajectories for each combination of simulation domains (n = 28), forest-type group (n = 3 to

235   10), and productivity class (n = 2). Forest type group is specified at a 0.01 degree resolution

236   obtained from *Zhu and Evans* [1994] (http://www.fia.fs.fed.us/library/maps/). Grid cell-level

237   fractions of forest land in high and low productivity classes for each forest type and stand age

238   within each region are specified from county level FIA data.

239   We modified CASA to capture disturbance impacts on the carbon cycle as follows. The post-

240   disturbance decline and ensuing recovery of *NPP* and fractional allocation to wood (τ) are

241   modeled as:

242

243      $$NPP(t) = NPP_{max}(1\text{-}c\mathrm{e}^{\text{-}kt})$$ (4),

244

245      $$\tau = min[1, (t-1)/8 \text{ years})]/3$$ (5),

246

247   where t is years since disturbance, NPP_{max} is the climatologically averaged net primary

248   productivity independent of a disturbance legacy, c (=1.5) determines the magnitude of

249   disturbance-induced reduction in NPP, k (=0.8) determines the rate of NPP recovery, and min is

250   the minimum operator. We introduced this dynamic recovery of NPP after disturbance based on

251   the well documented recovery of NPP [e.g. *Amiro et al.*, 2000; *Hicke et al.*, 2003]. The dynamics

252   of allocation were intended to capture initial investment of NPP into herbaceous biomass with

253   increasing allocation to woody vegetation with age [e.g. *Jokela et al.*, 2004; *Law et al.*, 2002].

254   In order to parameterize the amount of biomass killed by a disturbance we adopt the following

255   treatment. Regardless of the pre-disturbance biomass, we set the post-disturbance biomass to

256   50% of the aboveground live wood biomass reported in the 0-20 year age class. This constrains

257   early regrowth to pass through the youngest age-class in the FIA sample. We then estimate the

258   corresponding fraction of live wood, leaves, and roots killed based on the ratio of their abundance

259   prior to disturbance relative to those immediately after disturbance. Eighty percent of the

260   disturbance-killed aboveground wood and all of the disturbance-killed leaves are assumed to be

261   taken off site and entrained into wood products or promptly combusted and are collectively

262   accounted for as "removals" (fire and harvest), akin to the treatment by *Turner et al.* [1995]. The

263   remaining 20% of disturbance-killed aboveground wood is subject to on-site post-disturbance

264   decomposition as it enters the coarse woody debris pool, also consistent with *Turner et al.* [1995].

265   Disturbance-killed roots decompose on-site, for which 30% of dead coarse roots are assumed to

266   enter a belowground coarse woody debris pool, and 70% of dead coarse roots and all dead fine

267   roots enter the soil metabolic and structural pools, broadly consistent with results presented in

268   [*Gough et al.*, 2007; *Meigs et al.*, 2007]. We note that these and other prescriptions are uncertain,

269   likely vary among disturbance and forest types, and are the subject of ongoing research. In

270   summary, biomass killed in a disturbance event is the difference between pre-disturbance biomass

271   and 50% of the 0-20 year biomass reported by the FIA data. Of the killed biomass, 80% of

272   aboveground wood and all leaves are removed (via harvest or fire) and 20% of the killed

273   aboveground wood enters the coarse woody debris pool. The belowground wood and roots killed

274   by disturbance remain on site to decompose. Figure 3 offers an example, in which aboveground

275   biomass is reduced to 2.5/30 kg C m^{-2}, or <10%, and 80% of this 90% reduction in biomass is

276   assumed to be removed (harvest or fire) while the other 20% is left to decompose on site.

277   With this approach it is then possible to estimate biomass removals as:

$$R = A_1 B_{pre}(1 - f_{left})$$ (6),

279   where A_1 is the area of forested land assigned a stand age of one year based on the FIA age

280   histogram, B_{pre} is the pre-disturbance aboveground biomass, and f_{left} (=0.8) is the fraction of

281   biomass left to decompose on-site. Each of these varies by forest type, region, and productivity

282   class. This estimate is subject to errors in the area of forest assigned to this young age class, the

283   age of forests prior to disturbance and correspondingly the biomass pre-disturbance, and

284   uncertainty in the fraction of biomass in disturbed forests that is taken off-site as wood products.

285   Removals from non-stand replacing harvests are not considered in this approach but later in the

286   Discussion section we attempt to quantify the impacts of this assumption.

287   The next step in our model parameterization involves calculating the wood production – wood

288   age pair that allows the best match to the inventory data of aboveground stock recovery, with the

289   following multi-step procedure. First, we calculate a target aboveground live wood biomass (B^*,

290   in g C m^{-2}) from the mean in the 100 to 200 year old age classes, including successively younger

291   age classes in 20 year increments to ensure a minimum of two samples. The target age (A^*, in

292   years) is obtained from the average of old classes sampled to derive B^*. Second, we approximate

293   the rate of annual aboveground live wood biomass production (P_w, in g C m^{-2} a^{-1}), which is a

294   function of *NPP* and wood allocation, that would be required to obtain B^* by A^* for a range of

295   possible wood turnover times (A_w) spanning 30 to 300 years in increments of 10 years by solving

296   a simplified integral form of the differential equation for biomass with time ($dB/dt = P_w - B/A_w$) to

297   yield:

298

299
$$P_w = \frac{B^*}{A_w(1 - e^{\frac{-A^*}{A_w}})}$$
(7).

300

301   Thus, we obtain an array of possible P_w-A_w pairs that would grow the target biomass by the target

302   age. In a few particular cases this approach yielded implausible wood ages, but with negligible

303   consequence for the scales of analyses presented in this study. The third step is to select the pair

304   that provides a biomass recovery curve most like the inventory sample assessed as that which

305   minimizes the sum of squared error between modeled and sampled aboveground live wood

306   biomass. Modeled biomass is calculated at the sample ages (t, in years) according to:

307

308
$$B(t, A_w) = B_o e^{\frac{-t}{A_w}} + P_w A_w (1 - e^{\frac{-A^*}{A_w}})$$
(8),

309

310   where B_0 is an assumed initial biomass of 200 g C m^{-2}. Lastly, we linearly rescale the model's

311   default monthly *NPP* values to provide an annual total NPP_{max} inferred from the fitted rate of P_w,

312   as:

313
$$NPP_{max} = \frac{P_w}{\tau \alpha}$$
(9),

15

314   where τ (=1/3) is the allocation of *NPP* to wood and α (=0.75) is the fraction of this that is

315   allocated to the aboveground wood pool (stems and branches) instead of belowground (coarse

316   roots).

317   Following determination of P_w and A_w parameters, characteristic carbon flux trajectories

318   (Q_{afp}) are developed from, first, a 1000 year spin-up to steady-state carbon pools. This is followed

319   by a disturbance prior to the disturbance of interest with 75 years of regrowth for all forest types

320   except loblolly pine and longleaf / slash pine (30 years) and Douglas-fir (200 years). The age of

321   trees at harvest is set to be just older than the typical peak in age histograms reported by the FIA

322   (see Auxiliary 2, Figure A2.3), except where harvest rotations are known to be short (SE and SC

323   pines), or where harvest over previous decades tended to target old growth forests with high

324   economic value (Douglas-fir [*Cohen et al.*, 2002]). This 'pre-disturbance' is important in that it

325   establishes the amount of live carbon subject to disturbance-induced disposition, meaning taken

326   off-site as removals or decomposing on-site. Finally, we simulate the most recent disturbance

327   after which we allow 200 years of regrowth to characterize carbon dynamics with stand

328   development. These procedures result in a group of carbon stock age trajectories analogous to

329   yield tables.

330   We have not modified CASA's default treatment of heterotrophic respiration emerging from

331   microbial decomposition of soil and litter carbon and associated transfers among carbon pools.

332   The general equation for the rate of heterotropic respiration from a specific carbon pool is:

333

334   $$Rh_{pool} = C_{pool} k_{pool} W_{resp} T_{resp} M , \hspace{2cm} (10),$$

335

336   where C_{pool} is the amount of carbon in a pool, k_{pool} is the pool-specific decay rate constant, W_{resp}

337   and T_{resp} control how respiration depends on soil moisture and temperature states, and M is the

338   carbon assimilation efficiency of the microbes. Total heterotrophic respiration is the sum of that

339   from each of the nine detrital pools.

340

341   **2.3 Uncertainty Analysis**

342   A formal propagation of uncertainty from sampling errors (coefficient of variation, CV) for

343   forested area (±10 to 100%) and total aboveground live biomass (±10 to 100%), and volume to

344   carbon conversion (±7%) are all included. The uncertainty in inventory aboveground live

345   biomass per unit area is propagated to the predicted fluxes and aboveground live biomass with a

346   Monte Carlo procedure analogous to Tier 2 uncertainty estimation in the IPCC Good Practice

347   Guide [*IPCC*, 2000]. The model was fit to 25 different biomass regrowth trajectories, where each

348   trajectory was generated from random samples of the normally distributed aboveground live

349   wood biomass for each age class (25 draws of biomass per unit area from each of 10, 20-year age

350   classes). Forcing the fitted trajectory to conform to the assumption that biomass increases

351   monotonically and saturates with age strongly constrains the resultant age-accumulation curves

352   and their variances (Figure 3). An additional 7% uncertainty is used to account for tree volume to

353   carbon conversion [*Smith and Heath*, 2001]. Put together this method involved over 130,000

354   simulations of age-dependent dynamics of forest carbon fluxes and stocks. The uncertainty of

355   forest area and aboveground live biomass per unit area is obtained from the FIA data.

356   As shown in Equations 1-3 above, independent uncertainties in the product of flux or stock

357   with area are combined as $\delta Q_{total} = \left(\dfrac{\delta Q_{afp}^{\,2}}{Q_{afp}^{\,2}} + \dfrac{\delta A_{afp}^{\,2}}{A_{afp}^{\,2}} \right)^{1/2}$ [*Taylor*, 1997]. We adopt a conservative

358   assumption of non-random error propagation for which uncertainty is additive over forest types,

17

359   productivity classes, and ages, and also additive spatially for a simulation domain, a region, or the

360   nation. This uncertainty aggregation is analogous to a Tier 1 uncertainty described in the IPCC

361   Good Practice Guidance [*IPCC*, 2000].

362   Uncertainty in *NEP* also derives from model structure (not analyzed) as well as model

363   parameterization of light, moisture, and temperature sensitivity of heterotrophic respiration and/or

364   *NPP* expressed in the CASA model. As described in Auxiliary Material, Auxiliary 1 Section 1,

365   we analyzed *NEP* responses to a 2% increase of six representative parameters including the

366   maximum light use efficiency, moisture dependence of *NPP*, optimal temperature for *NPP*,

367   turnover time of the slow soil carbon pool, and both the Q10 and moisture dependence of

368   heterotrophic decomposition of soil carbon. We use a 2% change in parameter value in order to

369   obtain a detectable response in *NEP* but for ease of discussion the sensitivities are divided by two

370   and expressed as % change in *NEP* for a 1% change in parameter value (see Auxiliary Material,

371   Auxiliary 1).

372

373   # 3. Results

374   **3.1 Carbon Trajectories**

375   Using CASA as a controlled growth model accurately reproduces the accumulation of

376   aboveground forest carbon stocks with time since a stand replacing disturbance as informed by

377   FIA data (Figure 3), imposing a powerful, albeit partial, observational constraint on net ecosystem

378   carbon flux trajectories with stand age. Additional data on litter, woody debris and soil carbon

379   dynamics would provide much needed additional constraints on estimated ecosystem C dynamics.

380   More rapid regrowth of aboveground stocks in the high productivity class causes higher

381   amplitude trajectories for carbon stocks and fluxes (Figure A2.1, A2.2, Auxiliary 2) with larger

382 post-disturbance sources that give way to stronger sinks with ensuing forest regrowth. The Monte

383 Carlo simulation approach provides an envelope of trajectories (Figure 3) that enables formal

384 uncertainty propagation through all scales of the analysis (regional forest types to conterminous

385 U.S. forestlands). Absolute uncertainty surrounding *NEP* tends to peak where forest uptake is

386 maximum (peak *NEP*) and then diminishes with forest age (Figure 3). An important exception,

387 not shown in Figure 3, is the often large uncertainty in carbon emission in the years immediately

388 following disturbance; large because of variation in the pre-disturbance carbon stocks and the

389 amount of dead wood that decomposes on-site. The timing of *NEP* crossover from source to sink

390 is surprisingly insensitive to variability in biomass accumulation (not shown), and generally

391 occurs at ages <20 years (e.g. Figure 3 and Figure A2.1, A2.2, Auxiliary 2) consistent with many

392 reported chronosequence fluxes [e.g. *Bond-Lamberty et al.*, 2004; *Gough et al.*, 2007; *Goulden et*

393 *al.*, 2011; *Law et al.*, 2004; *Litvak et al.*, 2003; *Noormets et al.*, 2007; *Pregitzer and Euskirchen*,

394 2004]. Patterns of post-disturbance uptake of carbon in regrowing forests vary widely across

395 regions of the conterminous U.S. as well as by forest type group and productivity class (Figure

396 A2.1, A2.2, Auxiliary 2). Forest inventory data describing the recovery of aboveground live wood

397 biomass carbon with stand development act as a strong constraint on the modeled carbon cycle

398 including the rates of litter and soil carbon turnover and decay.

399   Our analysis of the sensitivity of the model to parameters revealed that nearly all of the

400 sensitivities are less than 1% indicating general dampening of parameter perturbations and

401 suggesting that uncertainties in these parameterizations do not expand as they propagate through

402 to modeled *NEP* (see Auxiliary 1, Table A1.1). Model structure and parameter uncertainties are

403 not included in our analysis but are expected to add about ±10% based partly on a sensitivity

404 analysis presented in Auxiliary Material 1.

405

3.2 Continental Patterns

407   Regional variations in disturbance rates and *NEP* across the conterminous U.S. reflect

408   harvesting practices and regional climates (Tables 1 and Table A2.1, Figures A2.1, A2.2, A2.3).

409   Forests growing in relatively dry settings (e.g. Rocky Mountain South (RMS)) have low *NEP*,

410   contrasted by high carbon sequestration rates in the Pacific Southwest and Northwest, as well as

411   Southeastern and South Central regions (Table A2.1). The largest rates of disturbance, and the

412   largest sinks of carbon stimulated by forest recovery from recent disturbance ("regrowth sinks"),

413   are in Southeastern (SE), South Central (SC), and Pacific Northwest (PNW) regions. These

414   regional biologically driven sinks do not reflect net biome productivity because recovery

415   trajectories do not include the fate of disturbance-induced carbon removals such as carbon taken

416   offsite to lumber, pulp and paper mills or released promptly on-site by natural and anthropogenic

417   fires (see schematic in Figure 1). This is addressed further in the discussion where we present the

418   forest-to-atmosphere carbon exchange.

419   At the continental scale, the biological recovery sink (*NEP*) is estimated to be 164 ± 28 Tg C a^{-1}

420   (Table 1), or about 71 g C m^{-2} a^{-1} averaged for the 230 million hectares of forestland represented

421   here. Nearly all (84%) of this *NEP* sink results from net growth of live carbon stocks with only a

422   small fraction shared among soil carbon (6%), litter carbon (2%), and coarse woody debris (8%)

423   stocks (Table 2). Our sample includes 93% of the conterminous U.S. forestland, reported to be

424   250 million hectares [*EPA*, 2008]. Our analysis did not include the Northern Prairie States region

425   (~6% of total area and ~5% of total carbon) because the effort was originally connected to a

426   Landsat remote sensing analysis whose random sample did not draw Landsat scenes for this

427   region. As verification, our stand-age histograms by region generally correspond well with a

428   similar presentation of the same basic data as recently published by *Pan et al.* [2011]. Comparing

429   to regional statistics of forest area and live biomass reported in *EPA* [2008] we find good

430   correspondence overall (Table 1).

431   The estimated uncertainty arising from forest area, aboveground wood biomass, and

432   conversion of diameter measurements to volume and carbon produced relatively small uncertainty

433   estimates in our biomass and fluxes. This is partly due to the continuous, monotonically

434   increasing, and saturating growth form imposed by the process-model approach. This functional

435   form is more plausible than one that would allow abrupt increases and decreases in aboveground

436   live wood biomass with stand development (i.e. stand age) as are commonly found in the

437   inventory data when arrayed as a chronosequence (e.g. Figure 3, 110- 150 year biomass).

438   Imposing the model's growth form has the effect of filtering out some of the variance inherent in

439   chronosequence trajectories of biomass with stand age. Other uncertainties arising from model

440   structure and assumptions about disturbance severity/type, age, partial cutting, natural wood

441   turnover, and a possible age-related decline in productivity are evaluated by judging the impacts

442   of these factors on model output through sensitivity analyses (see Auxiliary 1, Section 2).

443   We used the 1km forest type map to produce a gridded map of *NEP* and its uncertainty (from

444   variances in FIA data) for the conterminous US (Figure 4). Within each region each forest type

445   considered was assigned the regional estimate of *NEP* for that forest type and region. Regional

446   forest *NEP* sinks range from >25 to 200 g C m^{-2} a^{-1} with eastern and western forests generally

447   ranging from 75 to 100 g C m^{-2} a^{-1}. The RMS region is predicted to be uniformly <50 g C m^{-2} a^{-1}.

448   The discontinuities conforming to state borders between West Virginia and Virginia and between

449   Washington and Idaho occur because the same forest types in each neighboring region have

450   regionally specific and different growth and disturbance rates.

451   As an independent evaluation of our predicted stocks and fluxes we compared our results with

452   five available studies on chronosequences for forest types in the conterminous US. These studies

453   sometimes do not include estimates of both fluxes and stocks for different aged forests and

454   estimates used various biometric and flux measurement approaches. The small number of sites

455   with available data, variability in the data, and issues of extrapolating fine scale measurements to

456   regional responses do not justify quantitative comparisons and demonstrate the need for more of

457   these types of measurements and for finer scale modeling. The results of these comparisons are

458   shown in Auxiliary 3, Figure A3.1. Agreement varies widely between the comparisons at the

459   different sites/regions.

460

461 **4. Discussion**

462   Comparing estimates of the conterminous U.S. forest *NEP* sink from multiple studies (Table

463   3) reveals a general separation between age-accumulation and stock-change methods. This

464   comparison spans estimates for the 1980s to more recent years (e.g. 2005-2006), but this may be

465   justified because atmospheric inversions seem to indicate a long term mean sink in North

466   America during the '80's and '90's but with large interannual variability [*Baker et al*., 2006].

467   Four of the six age dependent analyses that seek to represent carbon emissions and sequestration

468   with post-disturbance recovery provide lower estimates of the forest *NEP* sink when compared to

469   the four stock-change analyses, with 82 g C m^{-2} a^{-1} versus 154 g C m^{-2} a^{-1} averaged across their

470   respective studies, or 189 Tg C a^{-1} versus 354 Tg C a^{-1} when integrated across US forest area.

471   This is even true when process-oriented studies rely on forest inventory data to prescribe the rate

472   of aboveground carbon stock recovery with time, as well as the area of forest of different ages.

473   For example, regarding *NEP* alone we find general agreement with *Turner et al.* [1995] who

474   reported 203 Tg C a^{-1} compared to our estimate of 164 Tg C a^{-1}. In contrast, the *EPA* [2008]

475   stock-change estimate of forest *NEP* is twice as large as this study's age-accumulation result (335

476   compared to 164 Tg C a^{-1}, Table 2). The disparity between the stock-change method and these

477   other, age-accumulation results is likely due to large annual to decadal increases in stocks

478   measured in the inventory that then implies greater *NEP* (regrowth). What causes this general

479   disagreement remains unclear, though growth enhancement is a plausible explanation of the

480   difference, consistent with recent publications [*Cole et al.*, 2010; *Luyssaert et al.*, 2010;

481   *McMahon et al.*, 2010; *Thomas et al.*, 2009]. Effects of growth enhancement are implicit in the

482   stock-change method but not well incorporated in the age-accumulation methods that emphasize

483   effects of regrowth dynamics, even when these methods rely on inventory-derived

484   chronosequences to constrain biomass accumulation as in the present study (see Auxiliary 4 for

485   an illustration of this). There is also one study reported in Table 3 including only the effects of

486   climate and CO_2 fertilization based on an ensemble of models for the conterminous US [*Schimel*

487   *et al.*, 2000]. If this sink were added to the forest recovery (age-yield table) estimates the results

488   would be more in line with the stock change approach.

489   We note that the *EPA* [2008] estimate of total removals is 38% higher than that estimated with

490   our modeling approach (=162/117, Table 3). About half of the difference is due to elevated fire

491   emissions reported in *EPA* [2008], however this estimate is much higher than the rate of forest

492   fire emissions being reported elsewhere (e.g. *van der Werf et al.*[2010]). This difference

493   translates directly into the *NEP* estimated from the stock change method, and elevates the *EPA*

494   [2008] estimate by 20 TgC a^{-1} relative to the estimate from our approach. The *EPA* [2008] report

495   also estimates 25 TgC a^{-1} greater removals by harvest. There are two ways we could adjust our

496   methodology to try to match this rate of removal. We could either, a) increase the amount of

497   biomass removed by disturbances on average by increasing the age and hence biomass of

498   disturbed forests, b) increase the amount of biomass removed on average by removing a larger

499   fraction of pre-disturbance biomass and leaving less to decompose on site, or c) increase the area

500   of forests disturbed by increasing the young-aged fraction of forests if we believe the stand age

501   attribute offers a biased representation. All of these would increase removals but they would have

502   different effects on *NEP*. The first option would decrease *NEP* because more disturbance-killed

503   material would be left on-site to decompose and be emitted from forests. The second approach

504   would increase *NEP* because of reduced on-site decomposition. The third approach would

505   decrease *NEP* because a larger fraction of forested area would be concentrated at young stand

506   ages (<15 year old) where *NEP* is either a large negative value or near zero (Figures A2.1, A2.2).

507   And in the extreme case that we simply adjusted our *NEP* estimate upwards to cover the

508   difference in removals, the *EPA* [2008] estimate would still be 126 TgC a^{-1} higher than the

509   estimate emerging from our age-accumulation method.

510   A term-by-term comparison between stock changes reported from inventory methods and

511   those derived in the current study's age-accumulation approach indicates that a change in live

512   carbon stocks makes up a large portion of the difference in *NEP* estimated with the two methods

513   (Table 2). Annual increases in soil carbon, coarse woody debris, and litter pools are also

514   noticeably lower in the present analysis compared to those reported by the *EPA* [2008; 2010]

515   (Table 3). Because our method, necessarily, produces aboveground live wood biomass and forest

516   area estimates that are consistent with, or wholly derived from, the inventory itself (Table 1), our

517   relatively low estimate of annual changes in live stocks (Table 2) does not appear to be caused by

518   underestimation of a) stocks, or b) forest area. These differences translate to the full forest sector-

519   atmosphere net exchange, whereby the stock-change method estimates a much larger forest sector

520   C sink than obtained with this study's age-accumulation approach (Table 2).

521   Our maps of conterminous US forest *NEP* and its uncertainty (Figure 4) are one of the first of

522   which we are aware (though see *Woodbury et al.* [2007]) and will be used in further study of the

523   impact of the forest disturbance fluxes on atmospheric CO_2 as a boundary flux for atmospheric

524   transport models much as gridded fire, fossil fuel burning, and ocean CO_2 fluxes are prescribed in

525   forward and inverse atmospheric modeling [e.g. *Peters et al.*, 2007]. Complete accounting of

526   forest sector fluxes would additionally require maps of fire [e.g. *van der Werf et al.*, 2010] and

527   wood products emissions. These studies will allow assessment of the detection limits for the

528   magnitude and spatial variability of sinks in top-down studies.

529   This study's approach imposed a number of simplifying assumptions that were necessary

530   given the initial scope of our work. Below we address some of these and their potential

531   implications regarding interpretation of our results.

532   • We assume characteristic regrowth trajectories regardless of disturbance type even though

533   the nature of post-disturbance carbon dynamics is sure to vary between fire, harvest,

534   hurricane, and the severity of disturbance. For instance, around twice as much coarse

535   woody debris (CWD) may remain on site after a severe fire compared to clear-cut harvest

536   [*Tinker and Knight*, 2000]. This remaining detritus provides a source of CO_2 for a

537   prolonged period after disturbance. Using data reported by *Smith et al.* [2009] and the

538   National Interagency Fire Center (to account for Alaskan fires) we estimate that for the year

539   2004 the ratio of burned area to harvested area in the eastern US was about 0.30 compared

540   to 0.46 in the west. In terms of carbon removals though, our forest fire estimates from the

541   Global Fire Emissions Database v3 (10 Tg C a^{-1}) are much smaller than our estimated

542   harvest removals (107 Tg C a^{-1}). Because the total removals are dominated by harvest, as is

543   the total area disturbed, accounting for differences caused by fire versus harvest would not

544   significantly change our results or conclusions. Furthermore, some but not all of this

545   variation is captured by the Monte Carlo approach, as well as with stratification by site

546   productivity and across regions. Partial disturbances such as defoliation events are not

547   represented with the current methodology, and discussed further below.

548   • Our assumption of equivalence between forest age and time since disturbance does not

549   account for the effects of partial disturbance that allows older aged trees to remain among

550   regenerating cohorts or the dynamic state of old forests that have reached the age of natural

551   mortality and reestablishment. This particular issue has been examined by *Bradford et al.*

552   [2008] for a subalpine forest system. In that study a large part of the age versus years since

553   disturbance discrepancy arose in stands undisturbed for long periods of time (>200 years),

554   longer than what we analyze in this work. From FIA data we estimate that about 3% of

555   forested land is >200 years old for conterminous US.

556   • Our analysis is sensitive to biases in the ages associated with the aboveground live wood

557   biomass trajectories, as explored in an extensive sensitivity analysis described in Auxiliary

558   1, Section 2. For instance, if the FIA ages are older (younger) than actual stand ages, our

559   predicted recovery sink is underestimated (overestimated). This, of course, is an issue with

560   any approach proposing to use FIA age structure information to estimate fluxes and stocks

561   [e.g. *Pan et al.*, 2011]. Despite this sensitivity, we note that bias in stand age is not likely to

562   be large enough to explain the major differences between the stock-change and age-

563   accumulation methods (Table A1.2).

564   • The FIA data we used to construct aboveground live wood biomass trajectories include the

565   effects of partial cuts, which are a significant component of disturbance in US forests

566   contributing >50% of the total harvested area [*Smith et al.*, 2009]. Reported stand ages

567   reflect the trees not cut while the plot level biomass will be lower in these cases producing

568   lower regional aboveground live wood biomass for mid and older aged stands. These partial

569   cutting practices (e.g. salvage logging, selective logging, thinning), which remove biomass

570   from forested plots without resetting the FIA-recorded stand age, could have a substantial

571   influence on the forest *NEP* estimate. The implicit inclusion of plots that experienced

572   partial cutting (not fully stocked) likely results in correct biomass estimates but lowers the

573   slope of regrowth trajectories resulting in some underestimation of *NEP*. In an extensive

574   sensitivity analysis (Auxiliary 1, Section 2) we find strong sensitivity to such biases, with a

575   10% elevation of biomass leading to a 14% elevation of conterminous US forest *NEP*. This

576   is equivalent to a 2.3 Tg C a^{-1} increase in *NEP* for each 1% increase in biomass. Despite

577   this large sensitivity to biomass trajectories, to account for the approximately 160 Tg C a^{-1}

578   difference, the reported biomass would need to have been underestimated by 70% (=160 Tg

579   C a^{-1} / 2.3 Tg C a^{-1} per 1% increase in biomass). Additional sensitivity analyses examining

580   effects of natural, partial disturbances that lead to wood turnover and on site decomposition

581   (e.g. ice storms, blowdowns, insect damage) indicate that they are also unlikely to present a

582   large error/bias in our estimate.

583   • We do not take into account annual changes in forest area which could contribute to the

584   discrepancy between recovery and stock change approaches. The *EPA* [2008] reports

585   indicate that forest area has been increasing at a rate of 0.24% a^{-1} since 1990. If we assume

586   that new forests would range between 1 to 5 kg C m^{-2} over an age range of 0 to 20 years

587   (e.g. see Figure 3) then the average accumulation rate for these forest would be about 250 g

588   C m^{-2} a^{-1}. Correcting this for the increase in forest area produces an added 1.7 Tg C a^{-1} sink,

589   indistinguishable within the uncertainties of our method.

590 • It has been proposed that forest carbon sinks may be driven by long term trends in

591   temperature, precipitation, nitrogen deposition, and atmospheric CO_2. Responses to these

592   trends are embedded in the biomass-age trajectories from the inventories in complex ways

593   and more recent increases in growth may not be accounted for in our approach (see

594   Auxiliary 4 for a thorough examination of this). Others have addressed this and concluded

595   that forests are not responding in a systematic way to these trends [*Caspersen et al.*, 2000],

596   that forest inventory data are not precise enough to resolve expected responses to trends

597   [*Joos et al.*, 2002], and that a smaller number of inventory measurements on forests of

598   known disturbance history do indeed show strong trends in growth enhancement correlated

599   with trends in temperature and atmospheric CO_2 [*McMahon et al.*, 2010; *Thomas et al.*,

600   2009]. In a study of global terrestrial carbon sinks using CASA, *Thompson et al.* [1996]

601   showed that in order to obtain a terrestrial carbon sink of ~2 Pg C/yr broadly consistent with

602   top-down sink estimates, *NPP* has to undergo a sustained increase of 0.18% per annum.

603   Similar estimates have been reported by others [e.g. *Joos et al.*, 2002]. Our own sensitivity

604   analysis (not shown) showed that a sustained increase in *NPP* of 0.2% per annum would

605   increase live biomass in a typical 60 year old forest by approximately 5% and is thus a weak

606   or undetectable signal in a biomass chronosequence. A 0.2% annual increase in *NPP* is

607   implausibly large sensitivity of photosynthesis to CO_2 (*dNPP/NPP* x CO_2/*d*CO_2 of ~0.96, or

608   near proportional response) and would require other positive feedback mechanisms such as

609   nitrogen fertilization and/or climate trends to operate in parallel. We conclude that plausible

610 responses of forest sinks to climate and CO_2 or N cannot be resolved with FIA biomass-age

611   trajectories alone such as those we utilize here and that have been proposed by others [e.g.

612   *Pan et al.*, 2011].

613 The approach described here is also sensitive to uncertain parameters including rates of wood

614 mortality and coarse woody debris decomposition, as well as the amount of dead aboveground

615 and belowground biomass left to decompose onsite following disturbance. It lacks a standing

616 dead wood pool that may be important because it decomposes much more slowly than dead wood

617 in contact with the forest floor [e.g. *Harmon and Hua*, 1991; *Harmon et al.*, 2004; *Janisch et al.*,

618 2005]. In our ongoing efforts, literature is being exhaustively explored to better constrain these

619 and other parameters and processes. Additional effort is being invested in attributing disturbances

620 to particular drivers based on spatial and geospatial records of fire and insect outbreaks. While

621 valuable, it is unlikely that such refinements and constraints will reconcile the large differences

622 between the age-accumulation and stock-change approaches, something that may benefit from a

623 close collaboration with inventory experts to clarify differences of approach and accounting, as

624 well as more comprehensive assessment of possible growth enhancement effects. Future efforts

625 at improving this study's approach will include more detailed prescriptions of type and severity of

626 disturbances, further comparisons with site observations as they become available, and analyses

627 of top-down atmospheric constraints on source/sink magnitude and distributions.   Estimates

628 would also be better constrained if additional data on litter, dead wood and soil organic carbon

629 dynamics were available from field studies.

630 5. Conclusions

631 Forest Inventory and Analysis data provide unique and valuable information about

632 disturbance history and associated carbon stocks and fluxes with forest recovery. By using these

633   data to constrain forest growth rates in a carbon cycle model, this study provides a more detailed

634   estimate of carbon sources and sinks from recent forest disturbance and recovery across regions

635   and forest types of the US. One of our key findings is a much smaller net sink of carbon in

636   conterminous US forests than previously estimated with the stock-change approach as used in

637   UNFCCC reporting [*EPA*, 2008]. The source of across study inconsistencies among national

638   estimates of stocks and fluxes remains largely unexplained. The paucity of observed net

639   ecosystem productivity and biomass chronosequences limits our ability to evaluate modeled

640   responses. These types of observations are critically needed in order to adequately test models

641   representing disturbance and subsequent recovery.

642

649 **References**

650 Adler, R., et al. (2003), The Version-2 Global Precipitation Climatology Project (GPCP) monthly

651   precipitation analysis (1979-present), *Journal of Hydrometeorology*, *4*(6), 1147-1167.

652 Amiro, B. D., et al. (2000), Net primary productivity following forest fire for Canadian

653   ecoregions, *Canadian Journal of Forest Research-Revue Canadienne De Recherche*

654   *Forestiere*, *30*(6), 939−947.

655 Amiro, B. D., et al. (2011), Ecosystem carbon dioxide fluxes after disturbance in forests of North

656   America, *Journal of Geophysical Research*, *115*, G00K02.

657 Baker, D. F., et al. (2006), TransCom 3 inversion intercomparison: Impact of transport model

658   errors on the interannual variability of regional CO2 fluxes, 1988-2003, *Global*

659   *Biogeochemical Cycles*, *20*, GB1002, doi:1010.1029/2004GB002439.

660 Barford, C., et al. (2001), Factors controlling long-and short-term sequestration of atmospheric

661   CO2 in a mid-latitude forest, *Science*, *294*, 1688-1691.

662 Bechtold, W. A., and P. L. Patterson (2005), The enhanced Forest Inventory and Analysis

663   program—national sampling design and estimation procedures, SRS GTR-80, USDA Forest

664   Service, Southern Research Station, Asheville, North Carolina, USA.

665 Birdsey, R. A., and L. S. Heath (1995), Carbon changes in U.S. forests, in *Productivity of*

666   *America's Forests and Climate Change*, edited by L. A. Joyce, Fort Collins.

667 Bond-Lamberty, B., et al. (2004), Net primary production and net ecosystem production of a

668   boreal black spruce wildfire chronosequence, *Global Change Biology*, *10*, 473-487.

669 Bousquet, P., et al. (2000), Regional changes in carbon dioxide fluxes of land and oceans since

670   1980, *Science*, *290*(5495), 1342-1346.

671   Bradford, J. B., et al. (2008), Tree age, disturbance history, and carbon stocks and fluxes in

672   subalpine Rocky Mountain forests, *Global Change Biology*, *14*, 2882-2897.

673   Caspersen, J. P., et al. (2000), Contributions of land-use history to carbon accumulation in US

674   forests, *Science*, *290*(5494), 1148-1151.

675   Chapin III, F. S., et al. (2006), Reconciling carbon-cycle concepts, terminology, and methods,

676   *Ecosystems*, *9*, 1041-1050.

677   Cohen, W., et al. (2002), Characterizing 23 years (1972-95) of stand replacement disturbance in

678   western Oregon forests with Landsat imagery, *Ecosystems*(122-137).

679   Cole, C. T., et al. (2010), Rising concentrations of atmospheric CO_2 have increased growth in

680   natural stands of quaking aspen (*Populus tremuloides*), *Global Change Biology*, *16*, 2186-

681   2197.

682   EPA (2008), Inventory of U.S. Greenhouse Gas Emissons and Sinks: 1990-2006, United States

683   Environmental Protection Agency, edited, Washington, DC.

684   EPA (2010), Inventory of U.S. Greenhouse Gas Emissons and Sinks: 1990-2008, United States

685   Environmental Protection Agency, Washington, DC.

686   Fan, S., et al. (1998), A large terrestrial carbon sink in North America implied by atmospheric and

687   oceanic carbon dioxide data and models, *Science*, *282*, 442-446.

688   Gough, C. M., et al. (2007), The legacy of harvest and fire on ecosystem carbon storage in a

689   northern temperate forest, *Global Change Biology*, *13*, 1935-1949.

690   Goulden, M. L., et al. (2011), Patterns of NPP, GPP, respiration, and NEP during boreal forest

691   succession, *Global Change Biology*, *17*, 855-871.

692   Goward, S. N., et al. (2008), Forest disturbance and North American carbon flux, *EOS*

693   *Transactions, American Geophysical Union*, *89*(11), 105-106.

694   Gurney, K. R., et al. (2002), Towards robust regional estimates of CO2 sources and sinks using

695   atmospheric transport models, *Nature*, *415*(6872), 626-630.

696   Hansen, J., et al. (1999), GISS analysis of surface temperature change, *Journal of Geophysical*

697   *Research*, *104*, 30997-31022.

698   Harmon, M. E., and C. Hua (1991), Coarse woody debris dynamics in two old-growth

699   ecosystems, *BioScience*, *41*(9), 604-610.

700   Harmon, M. E., et al. (2004), Production, respiration, and overall carbon balance in an old-growth

701   Pseudotsuga-Tsuga forest ecosystem, *Ecosystems*, *7*, 498-512.

702   Hicke, J. A., et al. (2003), Postfire response of North American boreal forest net primary

703   productivity analyzed with satellite observations, *Global Change Biology*, *9*(8), 1145-1157.

704   Houghton, R. A. (1999), The annual net flux of carbon to the atmosphere from changes in land

705   use 1850-1990, *Tellus Series B-Chemical and Physical Meteorology*, *51*(2), 298-313.

706   Houghton, R. A., et al. (1999), The US carbon budget: Contributions from land-use change,

707   *Science*, *285*(5427), 574-578.

708   Houghton, R. A. (2003), Why are estimates of the terrestrial carbon balance so different?, *Global*

709   *Change Biology*, *9*(4), 500-509.

710   Hurtt, G. C., et al. (2002), Projecting the future of the US carbon sink, *Proceedings of the*

711   *National Academy of Sciences of the United States of America*, *99*(3), 1389-1394.

712   IPCC (2000), Intergovernmental Panel on Climate Change Good Practice Guidance and

713   Uncertainty Management in National Greenhouse Gas Inventories, Institute for Global

714   Environmental Strategies, Japan.

715   Ito, A., et al. (2008), Can we reconcile differences in estimates of carbon fluxes from land-use

716   change and forestry for the 1990s?, *Atmos. Chem. Phys.*, *8*, 3291-3310.

717 Janisch, J. E., et al. (2005), Decomposition of coarse woody debris originating by clearcutting of

718   an old-growth conifer forest, *Ecoscience*, *12*(2), 151-160.

719 Jokela, E. J., et al. (2004), Production dynamics of intensively managed loblolly pine stands in the

720   southern United States: a synthesis of seven long-term experiments, *Forest Ecology and*

721   *Management*, *192*, 117-130.

722 Joos, F., et al. (2002), Growth enhancement due to global atmospheric change as predicted by

723   terrestrial ecosystem models: consistent with US forest inventory data, *Global Change*

724   *Biology*, *8*, 299-303.

725 Kaminski, T., et al. (2001), Inverse modeling of atmospheric carbon dioxide fluxes, *Science*, *294*,

726   259.

727 King, A. W., et al. (2007), The First State of the Carbon Cycle Report (SOCCR): The North

728   American Carbon Budget and Implications for the Global Carbon Cycle, *NOAA, National*

729   *Climatic Data Center, Asheville, NC*.

730 Koerner, C. (2003), Slow in, rapid out - carbon flux studies and Kyoto targets, *Science*, *300*,

731   1242-1243.

732 Law, B. E., et al. (2002), Environmental controls over carbon dioxide and water vapor exchange

733   of terrestrial vegetation, *Agricultural and Forest Meteorology*, *113*(1-4), 97-120.

734 Law, B. E., et al. (2003), Changes in carbon storage and fluxes in a chronosequence of ponderosa

735   pine, *Global Change Biology*, *9*, 510-524.

736 Law, B. E., et al. (2004), Disturbance and climate effects on carbon stocks and fluxes across

737   Western Oregon USA, *Global Change Biology*, *10*, 1429-1444.

738   Leemans, R., and W. P. Cramer (1991), The IIASA Database for Mean Monthly Values of

739   Temperature, Preicipitation and Cloudiness of a Global Terrestrial Grid, RR-91-18, 62 pp,

740   IIASA, Laxenburg, Austria.

741   Litvak, M., et al. (2003), Effect of stand age on whole ecosystem CO2 exchange in the Canadian

742   boreal forest, *Journal of Geophysical Research*, *108*(D3), 8225.

743   Luyssaert, S., et al. (2010), The European carbon balance. Part 3: forests, *Global Change Biology*,

744   *16*, 1429-1450.

745   McGuire, A. D., et al. (2001), Carbon balance of the terrestrial biosphere in the twentieth century:

746   Analyses of CO2, climate and land use effects with four process-based ecosystem models,

747   *Global Biogeochemical Cycles*, *15*(1), 183-206.

748   McMahon, S. M., et al. (2010), Evidence for a recent increase in forest growth, *Proceedings of*

749   *the National Academy of Sciences*, *107*(8), 3611-3615.

750   Meigs, G. W., et al. (2007), Forest fire impacts on carbon uptake, storage, and emission: The role

751   of burn severity in the Eastern Cascades, Oregon, *Ecosystems*, *12*, 1246-1267.

752   Myneni, R. B., et al. (2001), A large carbon sink in the woody biomass of Northern forests,

753   *Proceedings of the National Academy of Sciences of the United States of America*, *98*(26),

754   14784-14789.

755   Nemani, R., et al. (2002), Recent trends in hydrologic balance have enhanced the terrestrial

756   carbon sink in the United States, *Geophysical Research Letters*, *29*(10).

757   Nightingale, J. M., et al. (2009), Temporally smoothed and gap-filled MODIS land products for

758   carbon modelling: application of the fPAR product, *International Journal of Remote Sensing*,

759   *30*, 1083-1090.

760 Noormets, A., et al. (2007), Age-related changes in forest carbon fluxes in a managed northern

761   Wisconsin landscape, *Ecosystems*, *10*, 187-203.

762 Odum, E. (1969), The strategy of ecosystem development, *Science*, *164*, 262-270.

763 Pacala, S. W., et al. (2001), Consistent land- and atmosphere-based US carbon sink estimates,

764   *Science*, *292*(5525), 2316-2320.

765 Pan, Y., et al. (2009), Separating effects of changes in atmospheric composition, climate and

766   land-use on carbon sequestration of U.S. Mid-Atlantic temperate forests, *Forest Ecology and*

767   *Management*, *259*, 151-164.

768 Pan, Y., et al. (2011), Age structure and disturbance legacy of North American forests,

769   *Biogeosciences*, *8*, 715-732.

770 Peters, W., et al. (2007), An atmospheric perspective on North American carbon dioxide

771   exchange: CarbonTracker, *Proceedings of the National Academy of Sciences of the United*

772   *States of America*, *104*, 18925-18930.

773 Potter, C. S., et al. (1993), Terrestrial Ecosystem Production - a Process Model-Based on Global

774   Satellite and Surface Data, *Global Biogeochemical Cycles*, *7*(4), 811-841.

775 Pregitzer, K. S., and E. S. Euskirchen (2004), Carbon cycling and storage in world forests: Biome

776   patterns related to forest age, *Global Change Biology*, *10*, 2052-2077.

777 Randerson, J. T., et al. (1996), Substrate limitations for heterotrophs: Implications for models that

778   estimate the seasonal cycle of atmospheric CO2, *Global Biogeochemical Cycles*, *10*(4), 585-

779   602.

780 Richter, D. D., et al. (1999), Rapid accumulation and turnover of soil carbon in a re-establishing

781   forest, *Nature*, *400*, 56-58.

782   Schimel, D., et al. (2000), Contribution of increasing CO2 and climate to carbon storage by

783   ecosystems in the United States, *Science*, *287*(5460), 2004-2006.

784   Schimel, D. S., et al. (2001), Recent patterns and mechanisms of carbon exchange by terrestrial

785   ecosystems, *Nature*, *414*(6860), 169-172.

786   Schwalm, C. R., et al. (2007), A method for deriving net primary productivity and component

787   respiratory fluxes from tower-based eddy covariance data: a case study using a 17-year data

788   record from a Douglas-fir chronosequence, *Global Change Biology*, *13*, 370-385.

789   Smith, J. E., and L. S. Heath (2001), Identifying influences on model uncertainty: An application

790   using a forest carbon budget model, *Environmental Management*, *27*(2), 253-267.

791   Smith, W. B., et al. (2009), Forest Resources of the United States, *Gen. Tech. Rep. WO-78,*

792   *Washington, DC: USDA, Forest Service, Washington Office.*, 336p.

793   Stephens, B. B., et al. (2007), Weak northern and strong tropical land carbon uptake from vertical

794   profiles of atmospheric CO2, *Science*, *316*, 1732-1735.

795   Tans, P. P., et al. (1990), Observational Constraints on the Global Atmospheric Co2 Budget,

796   *Science*, *247*(4949), 1431-1438.

797   Taylor, J. R. (1997), *An introduction to error analysis: The study of uncertainties in physical*

798   *measuremnts 2nd ed.*, 326 pp., University Science Books, Sausilito, California.

799   Thomas, R. Q., et al. (2009), Increased tree carbon storage in response to nitrogen deposition in

800   the US, *Nature-Geoscience*, *3*, 13-17.

801   Thompson, M. V., et al. (1996), Change in net primary production and heterotrophic respiration:

802   How much is necessary to sustain the terrestrial carbon sink?, *Global Biogeochemical Cycles*,

803   *10*(4), 711-726.

804 Thornton, P. E., et al. (2002), Modeling and measuring the effects of disturbance history and

805   climate on carbon and water budgets in evergreen needleleaf forests, *Agricultural and Forest*

806   *Meteorology*, *113*(1-4), 185-222.

807 Tinker, D. B., and D. H. Knight (2000), Coarse woody debris following fire and logging in

808   Wyoming lodgepole pine forests, *Ecosystems*, *3*, 472-483.

809 Turner, D. P., et al. (1995), A carbon budget for forests of the conterminous United States,

810   *Ecological Applications*, *5*(2), 421-436.

811 van der Werf, G. R., et al. (2010), Global fire emissions and the contribution of deforestation,

812   savanna, forest, agricultural, and peat fires (1997-2009). *Atmos. Chem. Phys.*, *10*, 11707-

813   11735.

814 Woodbury, P. B., et al. (2007), Carbon sequestration in the U.S. forest sector from 1990 to 2010,

815   *Forest Ecology and Management*, *241*, 14-27.

816 Yang, Z., et al. (2007), New constraints on Northern Hemisphere growing season net flux,

817   *Geophysical Research Letters*, *34*(12), L12807.

818 Zhang, Y.-C., et al. (2004), Calculation of radiative fluxes from the surface to top of atmosphere

819   based on ISCCP and other global data sets: Refinements of the radiative transfer model and

820   the input data, *Journal of Geophysical Research*, *109*, D19105, doi:

821   19110.11029/12003JD004457.

822 Zheng, D., et al. (2011), Carbon changes in conterminous US forests associated with growth and

823   major disturbances: 1992-2001, *Environ. Res. Lett.*, *6*, 014012.

824 Zhou, L., et al. (2003), Relation between interannual variations in satellite measures of northern

825   forest greenness and climate between 1982 and 1999, *Journal of Geophysical Research-*

826   *Atmospheres*, *108*(D1).

827   Zhu, Z., and D. L. Evans (1994), US forest types and predicted percent forest cover from AVHRR

828   data, *Photogrammetric Engineering and Remote Sensing*, *60*, 525-531.

829
830

831   **Figure Captions.**

832   **Figure 1.** Schematic diagram illustrating stock and flux (italicized) relationships between the

833   forest sector and atmosphere. The entire forest sector net flux (sink) as defined by the stock-

834   change approach is: Net Flux = $\Delta\ C_{stocks}$ + $\Delta\ C_{wood\ products}$. Alternatively, using our model driven

835   estimates of *NEP* it is: Net Flux = *NEP – Wood Products Emissions – Fire*.

836   **Figure 2**. Conterminous U.S. distribution of forest type groups shown with thick state boundaries

837   that trace regions from the Resource Planning Act Assessment by the US Forest Service. Colors

838   differentiate FIA forest type groups. The rectangles represent areas where gridded climate and

839   phenology were used in the simulation of fluxes and stocks for each forest type within each

840   rectangle.

841   **Figure 3.** Characteristic trajectories of aboveground live wood biomass regrowth and associated

842   carbon sources / sinks (expressed as net ecosystem productivity, *NEP*) following a stand-

843   replacing disturbance in high productivity Douglas-fir stands of the Pacific Northwest. Results

844   are from the CASA model fit to regrow stocks consistent with 25 independent samples from the

845   forest inventory data (red circles). Net releases in the year following disturbance are as low as -

846   3000 g C m^{-2} a^{-1} (see Auxiliary Material 2, Figure A2.2) rising to above -500 g C m^{-2} a^{-1} in the

847   second year of regrowth.

848   **Figure 4a,b.** Map of average net ecosystem productivity (top, a) and uncertainty expressed as

849   one standard deviation (bottom, b) (*NEP* in g C m^{-2} a^{-1}) for forests of the conterminous US.

850

851

852   Table 1. Regional distribution of forest area, live biomass (Live B), ratio of EPA [2008] to this
853   study's forest area (f_{EPA08} Area), ratio of EPA [2008] to this study's live biomass (f_{EPA08} Live B),
854   net ecosystem productivity (NEP), fraction of forest that is less than 25 years old (<25y), less than
855   5 years old (<5y).

Region	Area	Live B	f_{EPA08}	f_{EPA08}	NEP	<25y	<5y
--	[10^9 m^2]	[Tg C]	Area [--]	Live B [--]	[Tg C a^{-1}]	[%]	[%]
NE	339	3,253	1.11	1.01	32±5.5	10	2
NLS	212	1,236	0.99	1.11	12±1.3	16	3
SE	355	2,621	1.00	0.94	30±3.5	39	8
SC	384	3,220	1.27	1.00	40±4.2	37	8
RMN	192	1,189	0.98	1.10	7±1.8	21	5
RMS	493	1,815	0.81	0.97	11±5.5	1	0
PSW	127	1,522	1.06	0.95	13±2.8	11	2
PNW	202	2,162	1.05	1.13	18±3.0	19	4
Total/Mean	2,303	17,017	1.03	1.08	164±27.7	17	4

856
857

858 Table 2. Changes in carbon stocks [Tg C a^{-1}] in the year 2005 reported in different studies.
859 Italicized values are inferred from mass balance.

	This Study	*EPA* [2008]
ΔTotal Soil C	3	9
ΔLitter C	1	15
ΔCoarse Woody Debris (CWD)	4	16
ΔCWD Below	0	--
ΔLive C	39	133
Total Stock Change	47	173
Removals[g]	117	*162*
Harvest[a]	*107*	132
Wildfire Emissions[b]	10	30
NEP[c]	164	*335*
Wood Products Emissions[d]	102	102
Wood Products Storage[e]	*5*	30
Forest Sector - Atmosphere Exchange[f]	52	203

860 [a]this study inferred as: Harvest = Removals – Wildfire Emissions;
861 [b]this study estimated wildfire emissions from the Global Fire Emissions Database v3 (GFED3)
862 [*van der Werf et al.*, 2010];
863 [c]for the purposes of this table calculated as:
864   *NEP* = ΔTotal Soil C + ΔLitter C + ΔCWD + ΔCWD Below + ΔLive C + Removals; values
865 differ from those in Table 1 due to differences in the method of aggregation and associated
866 averaging of terms;
867 [d]this study adopted values reported in *EPA* [2008];
868 [e]this study calculated as:
869   Wood Products Storage = Removals – Wood Products Emissions – Wildfire Emissions;
870 [f]this study calculated as:
871   Forest Sector-Atmosphere Exchange = *NEP* – Wood Products Emissions – Wildfire Emissions;
872 [g]for *EPA* [2008] calculated as: Removals = Wildfire Emissions + Harvest.

873   Table 3. Forest carbon *NEP* and stock change for the conterminous US [Tg C a^{-1}] from this and a

874   sample of previously published estimates. Estimates are classified according to approach: age

875   structure–C accumulation (*A&A*), stock change (ΔC_{stocks}=*NBP*), or process model (*P*), where *P* is

876   a process model ensemble result that accounts for CO_2 and climate effects [*Schimel et al.*, 2000],

877   and *Pacala et al.* [2001] combines approaches for an overall estimate and range. Low and High

878   refers to 1 standard deviation about the mean estimate.

Source	Approach	Mean *NEP*	Low	High	ΔC_{stocks}	Harvest	Fire
Schimel et al. [2000][a]	*P*	80					
This Study[b]	*A&A*	164	136	192	47	107	10
Houghton et al. [1999][c]	*A&A*	182			10	92	80
Turner [1995][e]	*A&A*	203			79	124	0
Houghton [2003][d]	*A&A*	207			35	92	80
Woodbury et al. [2007][f]	ΔC_{stocks}	270	256	293	108	132	30
EPA [2008][g]	ΔC_{stocks}	335			173	132	30
Birdsey & Heath [1995][h]	ΔC_{stocks}	368			211	127	30
Hurtt et al. [2002][i]	*A&A*	372	282	442	230	92	50
Pacala et al. [2001][j]	synthesis	392	312	472	220	92	80
King et al. [2007][k]	ΔC_{stocks}	411	383	439	236	145	30

879   a) for 1980-1993

880   b) for 2005, C stock change = *NEP – Harvest – Fire*, see Table 2, our total removals are 117

881   Tg C a^{-1} that includes fire and harvest, assume fire at 10 Tg C a^{-1} (see GFED3 of *van der*

882   *Werf et al.*[2010] and *Zheng et al.* [2011])

883   c) 1980s

884   d) for 1990's, harvest and fire from *Houghton et al.* [1999]

885   e) for ~1990,

886   f) for 2005

887   g) for 2005

888   h) for 1992

889   i) for 1980s

890   j) for 1980's

891   k) for 1980s

892

893 Figure 1. Schematic diagram illustrating stock and flux (italicized) relationships between the
894 forest sector and atmosphere. The entire forest sector net flux (sink) as defined by the stock-
895 change approach is: Net Flux = $\Delta C_{stocks} + \Delta C_{wood\ products}$. Alternatively, using our model driven
896 estimates of NEP it is: Net Flux = NEP – $Wood\ Products\ Emissions$ – $Fire\ Emissions$.
897

898
899
900

44
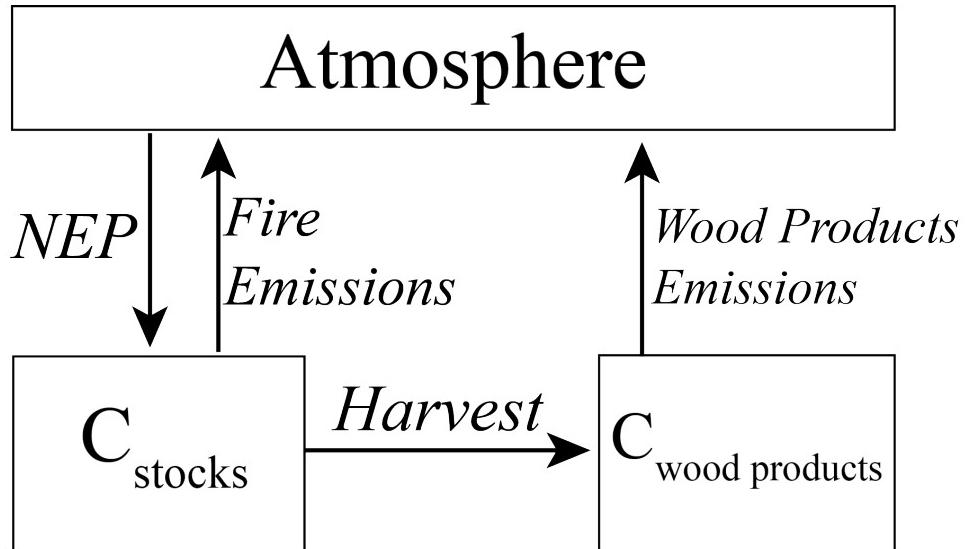
901   Figure 2. Conterminous U.S. Forest Type Groups shown with thick state boundaries that trace
902   regions from the Resource Planning Act Assessment by the US Forest Service. Colors
903   differentiate FIA forest type groups. The rectangles represent areas where gridded climate and
904   phenology were used in the simulation of fluxes and stocks for each forest type within each
905   rectangle.
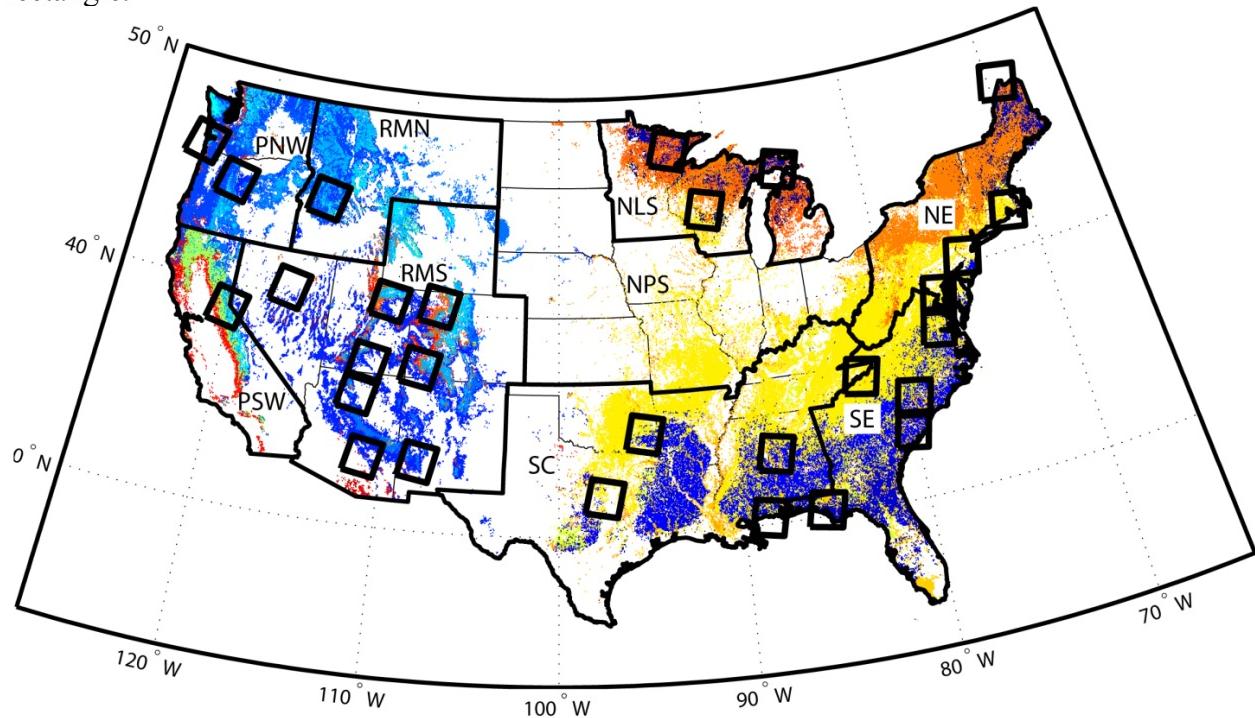

906
907
908
909
910
911

912   Figure 3. Characteristic trajectories of aboveground live wood biomass regrowth and associated
913   carbon sources / sinks (expressed as net ecosystem productivity, *NEP*) following a stand-
914   replacing disturbance in high productivity Douglas-fir stands of the Pacific Northwest. Results
915   are from the CASA model fit to regrow stocks consistent with 25 independent samples from the
916   forest inventory data (red circles). Net releases in the year following disturbance are as low as -
917   3000 g C m^{-2} a^{-1} (see Auxiliary Material 2, Figure A2.2) rising to above -500 g C m^{-2} a^{-1} in the
918   second year of regrowth.
919
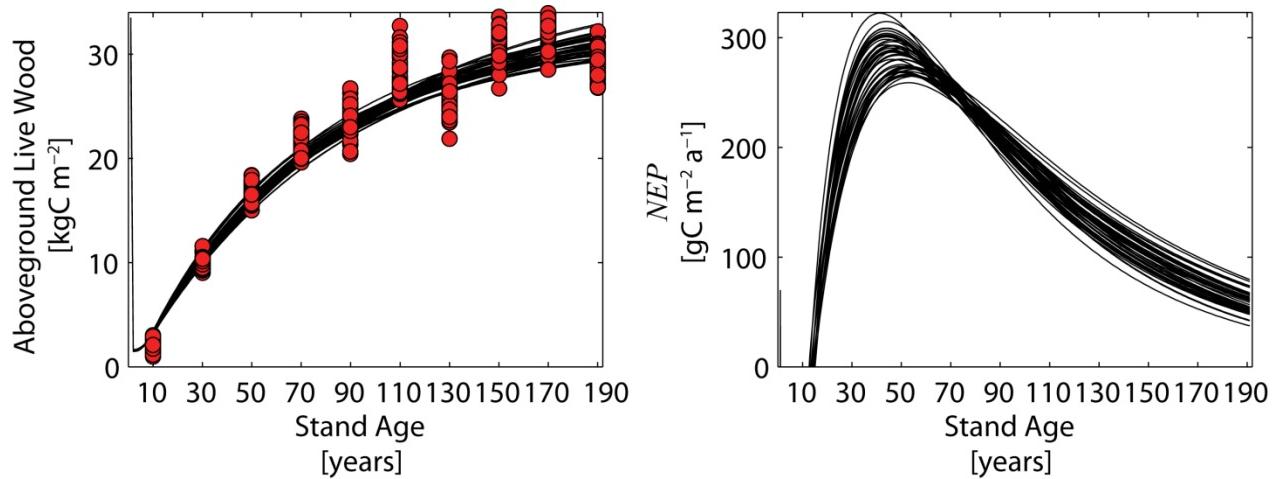
920

Figure 4a,b. Map of average net ecosystem productivity (top, a) and uncertainty expressed as one standard deviation (bottom, b) (*NEP* in g C m^{-2} a^{-1}) for forests of the conterminous US.